Adrenomedullin Induces Cardiac Lymphangiogenesis After Myocardial Infarction and Regulates Cardiac Edema Via Connexin 43

Claire E. Trincot, Wenjing Xu, Hua Zhang, Molly R. Kulikauskas, Thomas G. Caranasos, Brian C. Jensen, Amélie Sabine, Tatiana V. Petrova, Kathleen M. Caron

Rationale: **Cardiac lymphangiogenesis contributes to the reparative process post-myocardial infarction, but the factors and mechanisms regulating it are not well understood.**

Objective: **To determine if epicardial-secreted factor AM (adrenomedullin; *Adm*=gene) improves cardiac lymphangiogenesis post-myocardial infarction via lateralization of Cx43 (connexin 43) in cardiac lymphatic vasculature.**

Methods and Results: **Firstly, we identified sex-dependent differences in cardiac lymphatic numbers in uninjured mice using light-sheet microscopy. Using a mouse model of $Adm^{hi/hi}$ (*Adm* overexpression) and permanent left anterior descending ligation to induce myocardial infarction, we investigated cardiac lymphatic structure, growth, and function in injured murine hearts. Overexpression of *Adm* increased lymphangiogenesis and cardiac function post-myocardial infarction while suppressing cardiac edema and correlated with changes in Cx43 localization. Lymphatic function in response to AM treatment was attenuated in mice with a lymphatic-specific Cx43 deletion. In vitro experiments in cultured human lymphatic endothelial cells identified a novel mechanism to improve gap junction coupling by pharmaceutically targeting Cx43 with verapamil. Finally, we show that connexin protein expression in cardiac lymphatics is conserved between mouse and human.**

Conclusions: **AM is an endogenous, epicardial-derived factor that drives reparative cardiac lymphangiogenesis and function via Cx43, and this represents a new therapeutic pathway for improving myocardial edema after injury. (*Circ Res*. 2019;124:101-113. DOI: 10.1161/CIRCRESAHA.118.313835.)**

Key Words: adrenomedullin ■ connexin 43 ■ edema ■ endothelial cells ■ lymphatic vessels ■ myocardial infarction ■ sex characteristics

Lymphatic vascular circulation is essential for maintaining fluid dynamics, immune responses, and fat absorption. Defects in any aspect of lymphatic development or function can have dire effects in almost every organ system and in a large breadth of disease and injuries.[1,2] The heart has its own unique system of lymphatic vasculature consisting of an interconnected network of vessels covering the epicardial and subepicardial surface most densely concentrated surrounding the ventricles of the heart.[3] Cardiac lymphatics maintain the fluid homeostasis and immune response within the cardiovascular system.[4,5] Failure of these vessels to function properly and maintain a normal endothelial barrier can have profound consequences resulting in hypertension, inflammation, fibrosis, edema, and hemorrhage.[6–8] Recent work suggests a reactivation of these vessels after myocardial infarction (MI) may be the key to repair and scar tissue prevention by increasing cardiac function and prolonging survival.[9–11] However, precise factors that are endogenously expressed and induced after MI to drive this process remain to be elucidated.

Editorial, see p 15
Meet the First Author, see p 3

AM (adrenomedullin; *Adm*=gene), a known cardioprotective peptide, is essential for proper cardiovascular and lymphatic development in mice.[12] In murine studies, AM can stabilize the lymphatic endothelial barrier.[13] AM is clinically significant as well. In a pilot study, patients with acute MI received intravenous AM treatment and showed significant cardiovascular improvement.[14] Additionally, the BACH (Biomarkers in Acute Heart Failure) study and the Interdisciplinary Network Heart Failure program showed that mid-regional proAM, a cleaved form of AM, proved an

In September 2018, the average time from submission to first decision for all original research papers submitted to *Circulation Research* was 14.06 days.

From the Curriculum in Genetics and Molecular Biology (C.E.T., K.M.C.), Department of Cell Biology and Physiology (W.X., H.Z., M.R.K.), Division of Cardiothoracic Surgery, Department of Surgery (T.G.C.), Division of Cardiology (B.C.J.), Department of Medicine, School of Medicine (B.C.J.), McAllister Heart Institute (B.C.J., K.M.C.), and Department of Cell Biology and Physiology (K.M.C.), The University of North Carolina at Chapel Hill; Department of Oncology, University of Lausanne and Lausanne University Hospital and Ludwig Institute for Cancer Research Lausanne, Switzerland (A.S., T.V.P.); and Division of Experimental Pathlogy, Lausanne University Hospital (T.V.P.).

The online-only Data Supplement is available with this article at https://www.ahajournals.org/doi/suppl/10.1161/CIRCRESAHA.118.313835.

Correspondence to Kathleen M. Caron, PhD, Department of Cell Biology and Physiology, University of North Carolina at Chapel Hill, 111 Mason Farm Rd, MBRB 6312B, CB 7545, Chapel Hill, NC 27599. Email kathleen_caron@med.unc.edu

Novelty and Significance

What Is Known?

- Cardiac lymphatics proliferate in response to myocardial infarction (MI).
- Cardiac lymphatics may improve cardiac function and prevent the formation of scar tissue after MI.
- The cardioprotective peptide-adrenomedullin (AM) is expressed in lymphatic vessels.

What New Information Does This Article Contribute?

- Cardiac lymphatics differ between males and females.
- AM contributes to cardiac lymphangiogenesis post-MI.
- AM can regulate Cx43 (connexin 43), which may be vital for the proper functioning of cardiac lymphatics.

Cardiac lymphatics are new, potential therapeutic targets, especially in the context of MI. Although it is known that cardiac disease and injury affect men and women differently, sex differences in cardiac lymphatics have not been studied. Here we show that cardiac lymphatics develop differently in males and females, but in both sexes, AM can augment growth of cardiac lymphatics after MI, which contributes to increased cardiac function and less cardiac edema. We also found that within cardiac lymphatics both mice and humans express the same connexin proteins and that Cx43, a protein regulated by AM, contributes to the function of these vessels.

Nonstandard Abbreviations and Acronyms

AM	adrenomedullin
***Adm*$^{hi/hi}$**	adrenomedullin overexpression mouse
CLR	calcitonin receptor-like receptor
CFA	complete Freund's adjuvant
Cx43	connexin 43
hLECs	human lymphatic endothelial cells
GPCR	G-protein–coupled receptor
LECs	lymphatic endothelial cells
LYVE1	lymphatic vessel endothelial hyaluronan receptor 1
MI	myocardial infarction
RAMP2	receptor-activity modifying protein 2
VEGF	vascular endothelial growth factor
ZO-1	zonula occluden-1

effective diagnostic and prognostic tool and may be more sensitive than traditional biomarkers like natriuretic peptides in identifying high-risk patients.[15,16] Although, the upregulation of AM in disease states is well-appreciated, the downstream effectors and mechanism of action remain only partially understood.[17]

Cardiomyocytes must make connections with adjacent cells for communication of electrical impulses and propagation of contractions within the myocardium. Cx43 (connexin 43) is the most abundantly expressed connexin within the heart and is essential for normal cardiac conductivity.[18] Typically, 6 connexins oligomerize to form an opening or pore in the cell membrane known as a hemichannel.[19] When 2 hemichannels from adjacent cells oppose one another, they form a connection that links the cytoplasm of those 2 cells, known as a gap junction, named for the steric 2 to 3 nm gap that forms between cells at this junction.[20] Gap junction intercellular communication allows for the passage of small signaling molecules, ions, metabolites, ATP, prostaglandins, small peptides, miRNAs, etc to pass from 1 cell to another.[21–23] Given the role of Cx43 in cardiomyocyte contractility and cell-cell coupling, it has been highlighted as a potential therapeutic target.[24–26] Connexins and gap junctions are also critical in the proper development and maintenance of lymphatic function.[27] Lymphatic deletion of Cx43 leads to a delay in lymphatic valve initiation, improper lymphatic valve formation and function, altered lymphatic capillary patterning, and sometimes lethal chylothorax.[28] Not only are connexin proteins vital to proper lymphatic development, but they may affect mature lymphatics through paracrine signaling via hemichannels and gap junction intercellular communication.[29] Human mutations in connexin proteins lead to a variety of lymphatic disorders, including lymphedema.[30–32]

Although connexin proteins have been studied extensively within the context of cardiomyocytes and electrical conduction in the heart, there has been little work done to evaluate how connexins specifically contribute to the function and maintenance of cardiac lymphatic vasculature. For the first time, we characterize connexin protein expression patterns within the cardiac lymphatic vasculature both in murine and human heart tissue. In this study, we demonstrate a critical role for AM in lymphangiogenesis in the heart and how it may regulate Cx43 in cardiac lymphatics to improve cardiac function after MI.

Methods

The authors declare that all supporting data are available within the article and its online-only Data Supplement.

Animals

Adm$^{hi/hi}$ (*Adm* overexpression) mice were designed as described previously in which the targeting vector replaces the endogenous 3′ UTR (untranslated region) to stabilize the mRNA and increase half-life thus elevating *Adm* expression.[33] Genotyping was assessed using a standard polymerase chain reaction-based strategy with 3 primers: primer 1: 5′-AACCTTAC ACCTTGCTGAGACATTC-3′; primer 2: 5′-TTTATTAGGAAAGGACAGTGG GAGTG-3′; and primer 3: 5′CCCACATT CGTGTCAAACGCTAC-3′. Primers 1 and 3 amplify a 760-bp wild-type allele, while primers 2 and 3 amplify a 600-bp targeted allele. Mice used in these studies were backcrossed to C57Bl6 for over 9 generations. For all experiments, littermate animals or age-matched C57Bl6 wild-type males were used as controls. All mice used were 3 to 6 months of age (n=84 males; 33 females). Cx43 (Gja1 [gap junction protein alpha 1])-floxed (*Cx43*$^{fl/fl}$) mice[34] (mice strain no. 008039, Jackson Laboratories) were crossed with inducible Vegfr3-CreER (T2) mice[35] to produce *Vegfr3-CreER*^{T2}; *Cx43*$^{fl/fl}$. Cre-mediated recombination was induced by administering TAM (Sigma-Aldrich T5648) dissolved in corn oil and ethanol to mice aged 1 to 5 months (n=28) for 5 consecutive days at a dose of 10 µg/g intraperitoneally. Wild-type and Cx43-floxed allele polymerase chain reaction was determined by protocol provided by the Jackson Laboratory. Genotyping the Vegfr3-CreER (T2) allele was assessed using a

standard polymerase chain reaction-based strategy with 2 primers: primer 1: 5′ GGCTGGACCAATGTAAATATTG 3′ and primer 2: 5′ CATCATCGAAGCTTCACTG 3′ to amplify a 285-bp targeted allele. For all experiments, littermate animals or age-matched *Vegfr3*$^{+/+}$; *Cx43*$^{fl/fl}$ or *Vegfr3*$^{+/+}$; *Cx43*$^{fl/+}$ were used as controls. The animal study was in line with the guidelines and approved by the Office of Animal Care and Use at the University of North Carolina, Chapel Hill and complied with the National Institute of Health guidelines.

MI Model-Permanent Ligation of the Left Anterior Descending Coronary Artery

Mice were anesthetized using ketamine (100 mg/kg, im) and xylazine (15 mg/kg, im) and rectal temperature maintained at 37±0.5ºC. The trachea was cannulated with a 20 mm length of 18-gauge polyethylene tubing, followed by ventilation with a positive-pressure, constant-volume ventilator (model 845; Harvard Apparatus Co, South Natick, MA; stroke volume 200 µL, 150 strokes/min). A 3 mm left thoracotomy was performed between the third and fourth ribs to visualize the left anterior descending coronary artery. The proximal trunk of the left anterior descending was ligated with 7-0 silk suture. The muscle and skin incisions were closed with 6-0 and 5-0 suture, respectively, buprenorphine administered (40 µg/kg, sc) and the animal gradually weaned from the respirator.

Light-Sheet Microscopy

Adult murine hearts were fixed and stained using the iDISCO (immunolabeling-enabled three-dimensional imaging of solvent-cleared organs) method as described previously using rabbit anti-LYVE1 (1:500, Fitzgerald) primary antibody for 8 days and incubated with secondary donkey anti-rabbit AF647 (1:200, Thermo Fisher Scientific) for 8 days.[36] Samples were imaged using the Lavision Ultramicroscope II light-sheet system. Images were acquired with Imaris software.

Echocardiography

Conscious echocardiography was performed using VSI 2100 high-frequency ultrasound (VisualSonics) as previously described.[37]

Infarct and Fibrosis

Infarct size was assessed using traditional hematoxylin-eosin (H&E) histology and cardiac sections using a modified midline infarct size method as previously described.[38] Fibrotic area was measured by threshold level in Fiji and normalized to total area.

Scrape-Loading Dye Transfer

A confluent monolayer of human lymphatic endothelial cells (hLECs) was grown on coverslips. The scrape assay was performed as previously described.[39]

Quantitative Tail Microlymphography

Anesthetized adult *Vegfr3-CreER*^{T2}; *Cx43*$^{fl/fl}$ and control animals were injected in the tail with 10 µL of a 25% fluorescein isothiocyanate dextran (2 000 000 kDa) with a vehicle or AM peptide (10 ng/µL) as previously described.[13] The flow of fluorescein isothiocyanate dextran through dermal tail lymphatics was acquired with Leica MZ16FA dissecting stereoscope outfitted with a QImaging Micropublisher 5.0 RTV color charge-coupled device camera for several minutes postinjection using Metamorph software (Molecular Devices Corp). Analyses were performed using Fiji.

Edema Formation Assay

Anesthetized adult *Adm*$^{hi/hi}$ and control animals were injected with 10 µL of [4 µg/µL] of Complete Freund's Adjuvant (CFA) as described previously in one hind paw while the other paw served as a control.[40] Paw thickness was measured using calipers before CFA injection and every day after injection for 6 days.

Evans Blue Ear Injection

Ear lymphatic permeability was assessed as previously described.[40] Anesthesized adult *Vegfr3-CreER*^{T2}; *Cx43*$^{fl/fl}$ and control animals were injected intradermally with 3 µL 0.5% Evans Blue dye (Sigma-Aldrich) in saline with a 10 µL Hamilton syringe fitted with a 30 gauge needle. Images of the ears were acquired with Leica MZ16FA dissecting stereoscope outfitted with a QImaging Micropublisher 5.0 RTV color charge-coupled device camera using Metamorph software (Molecular Devices Corp) at 0, 5, and 15 minutes after injection.

Results

Sex-Dependent Differences in Cardiac Lymphatics

Using light-sheet microscopy, a method of imaging immunolabeled large, intact organs with a sheet or plane of light in contrast to traditional point laser light and staining for LYVE1 (lymphatic vessel endothelial hyaluronan receptor 1), we characterized the 3-dimensional structure and branching patterns of murine cardiac lymphatics (Figure 1A). Overall, the majority of the vessels appeared on the epicardial surface of the heart and densely cover both atria and ventricles. Many small capillaries branched from the larger collecting vessels. Vessels extended shallowly into the subepicardium and subendocardium but were notably absent from the myocardium of the ventricles. It has been shown that lymphatic capillary vessels exist in cardiac valve tissue, but the tissue is too opaque to visualize vessels within valves using this method.[41] To examine the vasculature further, we observed immunofluorescence of lymphatic marker LYVE1 in paraffin cross-sections through the ventricular wall (Figure 1B). Immunofluorescence staining allowed us to count individual vessels. Using this combination of techniques, we discovered sex-dependent differences in cardiac lymphatic vasculature. Regardless of genotype, female mice consistently had more lymphatic vessels within their heart (Figure 1C).

Given the distinct role of AM in cardiovascular and lymphatic development, we sought to characterize how overexpression of *Adm* affects the cardiac lymphatic vasculature in healthy adult mice. Male *Adm*$^{hi/hi}$ mice have approximately a 3-fold increase of AM in the heart compared with wild-type littermates.[42] Adult male mice with overexpression of *Adm* showed no obvious differences in cardiac lymphatic anatomy or density compared with respective wild-type littermates (Figure 1A and 1B). However, female *Adm*$^{hi/hi}$ mice have approximately a 60-fold increase of AM in the heart compared with wild-type littermates.[43] This further increase in AM resulted in more cardiac lymphatic vasculature and a denser plexus of vessels in female *Adm*$^{hi/hi}$ mice compared with age-matched wild-type mice (Figure 1A and 1B). The increase in the number of vessels was most visible at higher magnification of the ventricular wall. Quantification of cardiac lymphatic vessels confirmed that there was no genotype difference in the number of vessels between male mice (Figure 1C). Yet, female *Adm*$^{hi/hi}$ mice had significantly more cardiac lymphatic vessels than their wild-type counterparts (Figure 1C).

Adm Drives Cardiac Lymphangiogenesis in a Surgical Model of MI

It is known that cardiac lymphatics proliferate and remodel in response to injury.[9–11] Since AM is primarily secreted from the epicardium, we considered that it may promote cardiac lymphangiogenesis after injury.[42] Using permanent left anterior descending ligation, *Adm*$^{hi/hi}$ mice experience significantly more cardiac lymphatic growth than age-matched *Adm*$^{+/+}$ mice as quantified by counting all vessels positive for lymphatic marker LYVE1 15–21 days after MI in cross-sections through both ventricles (Figure 1D

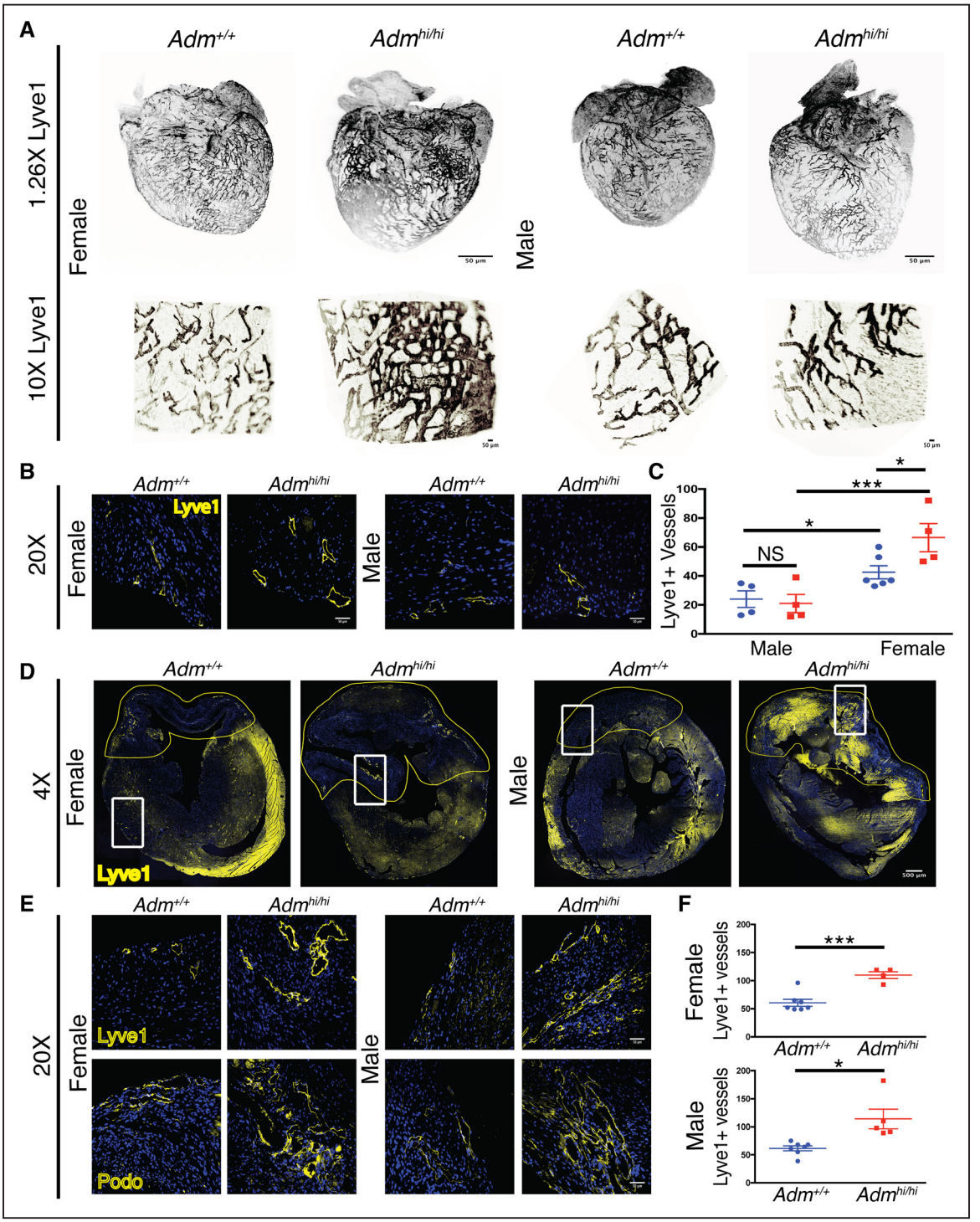

Figure 1. Adrenomedullin *(Adm)* drives sex-dependent cardiac lymphangiogenesis during development and surgical model of myocardial infarction (MI). A, Light sheet 3-dimentional (3D) microscopy for cardiac lymphatic vasculature in healthy adult male and female wild-type ($Adm^{+/+}$) and $Adm^{hi/hi}$ mice (black=LYVE1); scale bar=50 μm. **B**, Immunohistochemistry of cardiac sections in healthy adult male and female $Adm^{+/+}$ and $Adm^{hi/hi}$ mice (yellow=LYVE1, blue=Hoescht); scale bar=50 μm. **C**, LYVE1+ vessels/section in adult male mice (n=4 for all groups) and adult female mice (n=6 $Adm^{+/+}$; n=4 $Adm^{hi/hi}$) NS $P>0.05$, *$P<0.05$, ***$P<0.001$ by Uncorrected Fisher least significant difference 2-way ANOVA. **D**, Immunohistochemistry of cardiac sections in infarcted adult $Adm^{+/+}$ and $Adm^{hi/hi}$ mice 15–21 d post-MI (yellow=LYVE1, blue=Hoescht); scale bar=500 and 50 μm. Infarct zone is outlined and boxed zone is highlighted in panels below (**E**). **E**, (yellow=LYVE1, Podoplanin; blue=Hoescht); scale bar=50 μm. **F**, Quantification of LYVE1+ vessels 15–21 d post-MI (n=7 $Adm^{+/+}$; 4–5 $Adm^{hi/hi}$). *$P<0.05$, ***$P<0.001$ by unpaired Student 2-tailed *t* test with Welch correction. Mean±SEM is shown.

through 1F). Despite, increased numbers of cardiac lymphatic vessels by 15-days post-MI, male mice still had nearly equivalent number of vessels at 10-days post-MI (Figure I in the online-only Data Supplement). Lymphatic vessels were most concentrated in the peri-infarct zone, especially in $Adm^{hi/hi}$ mice. Comparing the number of lymphatic vessels before and after left anterior descending ligation, we saw that $Adm^{hi/hi}$ mice have a higher rate of lymphatic growth after injury (Figure 1F). Further characterization of

lymphatics in infarcted hearts using cardiac lymphatic vasculature marker podoplanin confirmed more lymphangiogenesis in *Adm*$^{hi/hi}$ mice with denser clusters of lymphatic vessels near the epicardial border zone (Figure 1E). Despite female mice having more cardiac lymphatics before injury (independent of genotype), after MI, both sexes had comparable numbers of lymphatic vessels with *Adm*$^{hi/hi}$ mice consistently having more cardiac lymphatic vessels than *Adm*$^{+/+}$ mice.

Overexpression of *Adm* Results in Less Edema and Dilated Cardiac Lvasculature Post-MI

Histology revealed that cardiac edema post-MI is concentrated on the surface of the ventricles in the peri-infarct zones, and we observed significant differences in the swelling and accumulation of fluid between the epicardial and subepicardial layers of the heart between genotypes, most prominently in the male mice (Figure 2A). The left ventricular wall overall had less thinning areas and more preserved myocardium muscle in *Adm*$^{hi/hi}$ male mice. Consistent with the appearance of the cardiac lymphatics, we found significant differences in the extent of cardiac edema between genotypes in male mice. *Adm*$^{hi/hi}$ male mice had significantly less cardiac edema 15 to 21 days after injury as assessed and scored via histology (Figure 2A and 2B). Consistent with the number of lymphatic vessels, at 10 days after injury, male mice do not yet have significant differences in cardiac edema, nor do the circumferential areas of the vessels differ (Figure I in the online-only Data Supplement). Female mice had no significant differences in cardiac edema 15 days after injury. It is possible that the acute, primary waves of edema were cleared more efficiently in female mice because of increased lymphatics during development, yet later stage edema was already stabilized. The difference we see in male mice may be residual clearing efficiency from the second wave of acute edema post-MI. Cardiac lymphatic vessels were dilated and increased in area in *Adm*$^{hi/hi}$ animals, both male and female, post-MI as quantified by measuring circumference of LYVE1 positive vessels in the ventricles of the heart. (Figure 2C and 2D). Microscopy revealed lymphatic vessels with more circular, patent lumens in *Adm*$^{hi/hi}$ mice compared with the thin, collapsed vessels of the age-matched wild-types (Figure 2C). To further assess edema clearance in mice overexpressing *Adm*, we injected the hind paws of both *Adm*$^{hi/hi}$ and *Adm*$^{+/+}$ mice with CFA to challenge the lymphatic vascular system with localized inflammation-induced edema. Both *Adm*$^{hi/hi}$ and control mice exhibited an immediate and significant increase in paw thickness within minutes of CFA injection that continued to worsen over 48 hours (Figure 2E). Overall, *Adm*$^{hi/hi}$ mice were significantly better at resolving edema. However, the timing of the resolution differed by sex, consistent with edema clearance in hearts post-MI. Female *Adm*$^{hi/hi}$ mice showed significantly less paw edema 1 day postinjection, while *Adm*$^{hi/hi}$ male mice began to alleviate edema between 2 and 3 days postinjection with significantly less edema by 6 days postinjection. We observed differences in timing of resolution even in control mice; female control mice began to slowly resolve edema by 3 days

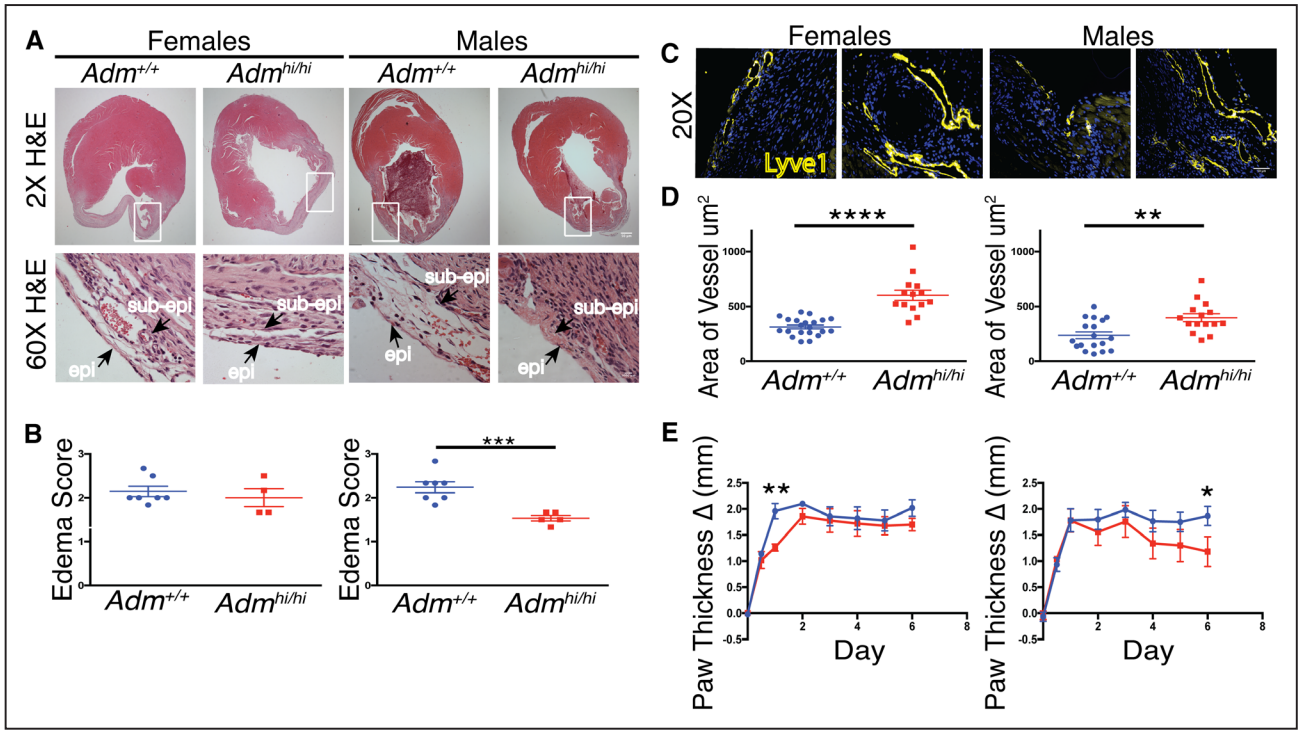

Figure 2. Overexpression of *Adm* results in less edema and dilated cardiac lymphatic vasculature post-myocardial infarction (MI). A, Histology hematoxylin-eosin (H&E) of cardiac sections 15–21 d post-MI with infarcted boxed area highlighted in panels below, with epicardial (epi) and subepicardial (sub-epi) layers highlighted with arrows; scale bar=50 and 1000 μm. **B**, Quantification of edema 15–21 d post-MI (n=7 *Adm*$^{+/+}$; 4–5 *Adm*$^{hi/hi}$). ***P<0.001 by unpaired Student 2-tailed t test with Welch correction. Mean±SEM is shown. Statistical significance (P=0.0013 in males; P>0.05 in females) is confirmed with nonparametric tests, Mann-Whitney U test and Kolmogorov-Smirnov. **C**, Immunohistochemistry of cardiac sections in infarcted adult *Adm*$^{+/+}$ and *Adm*$^{hi/hi}$ mice 15–21 d post-MI (yellow=LYVE1, blue=Hoescht); scale bar=50 μm. **D**, Quantification of vessel area (μm^2) 15–21 d post-MI (n=6–7 *Adm*$^{+/+}$; 5 *Adm*$^{hi/hi}$). **P<0.001, ****P<0.0001 by unpaired Student 2-tailed t test with Welch correction. Mean±SEM is shown. **E**, Quantification of paw thickness normalized to uninjected paw (mm) (n=5–6 *Adm*$^{+/+}$; 4–5 *Adm*$^{hi/hi}$). *P<0.05, **P<0.001 by unpaired Student 2-tailed t test with Welch correction. Mean±SEM is shown.

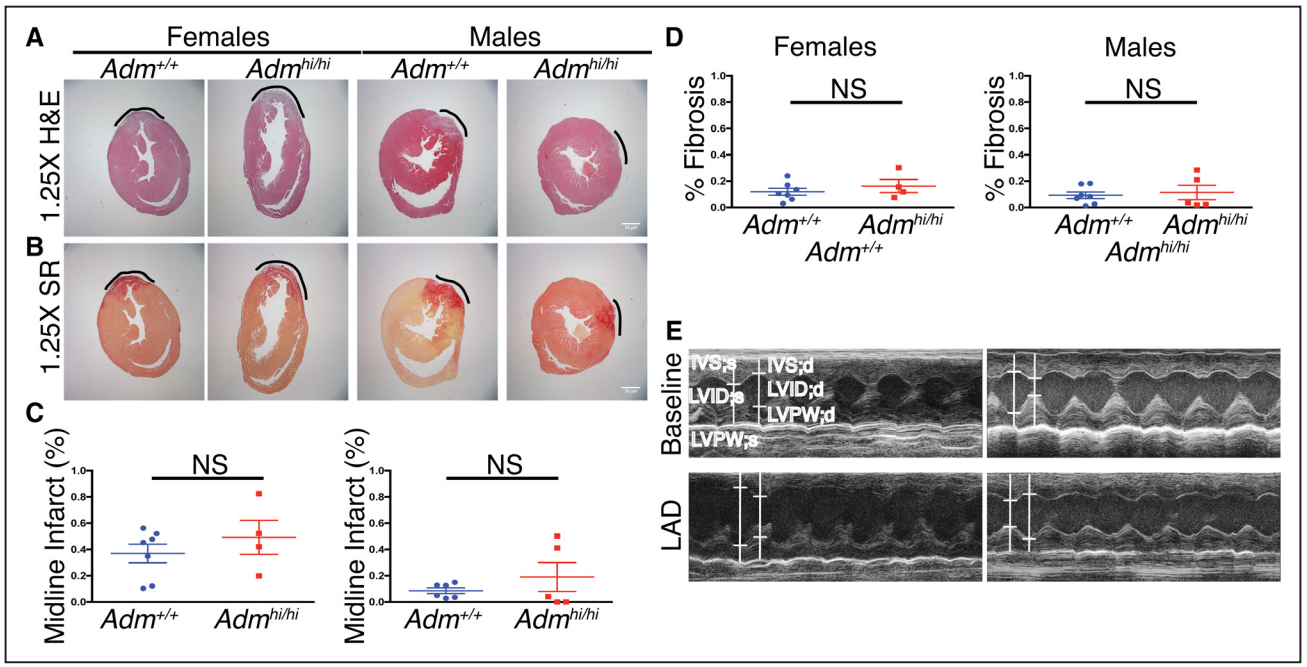

Figure 3. Overexpression of *Adm* correlates with improved cardiac function post-myocardial infarction (MI). A, Histology hematoxylin-eosin (H&E) with infarcted area outlined. **B**, Fibrosis picrosirius red (SR) of cardiac sections 15–21 d post-MI with fibrotic area outlined; scale bar=50 μm. **C**, Quantification of infarct size. **D**, Fibrotic area 15–21 d post-MI (n=7 $Adm^{+/+}$; 4–5 $Adm^{hi/hi}$) NS $P>0.05$, by unpaired Student 2-tailed *t* test with Welch correction. Mean±SEM is shown. **E**, Representative M-mode echocardiograms from left ventricles of $Adm^{+/+}$ and $Adm^{hi/hi}$ male mice before and after (15 days) MI with echo measurements labeled.

postinjection, while male control mice showed prolonged and exacerbated edema even 6 days postinjection.

Overexpression of *Adm* Correlates With Improved Cardiac Function Post-MI

Hematoxylin-eosin histology and Picrosirius red staining were used to characterize infarct size and fibrotic area 15 to 21 days after injury (Figure 3A and 3B). Hematoxylin-eosin was used to measure the infarct length normalized to total circumference (midline infarct). There was no significant difference in infarct size between genotypes in males or females (Figure 3A and 3C). Using H&E and Mason's Trichrome to measure infarcted area normalized to total area of the heart also showed no significant differences in infarct size (data not shown). Collagen deposition as evidenced by Picrosirius red staining showed no significant differences in fibrotic scar tissue between genotypes in males or females (Figure 3B and 3D). In male mice, we observed no significant differences in infarct size or fibrotic area 10 days after injury (Figure I in the online-only Data Supplement).

Despite the similarities in size of infarcted tissue, $Adm^{hi/hi}$ mice showed significantly improved cardiac function after MI. Uninjured $Adm^{hi/hi}$ mice and $Adm^{+/+}$ mice are functionally equivalent with no notable differences in either sex. Conscious echocardiography data, summarized in Tables 1 & 2, showed that ejection fraction and fractional shortening were significantly increased in $Adm^{hi/hi}$ mice 15 days after injury in males and 10 days after injury in females. Thus, the lymphangiogenesis and cardiac edema reduction seen in $Adm^{hi/hi}$ mice 2 weeks after injury appeared to have imparted significant improvement in the cardiac function compared with age-matched wild-type animals with the same amount of injury and damage. Overall, $Adm^{hi/hi}$ mice seem less dilated than wild-type animals. Representative M-mode echocardiograms show the dilation and remodeling post-MI in $Adm^{+/+}$ male mice (Figure 3E). These significant morphology changes observed in M-mode echocardiography were reflected in interventricular septal and left ventricular internal diameter measurements 15 days after injury in male mice.

Adm Affects Localization of Cx43 in Injured Myocardium

AM has previously been shown to regulate Cx43 in lymphatic endothelial cells (LECs).[39] To assess the role of AM in regulating Cx43, we used immunofluorescence to evaluate levels and localization of the protein in cross-sections of healthy, uninjured myocardium in both $Adm^{hi/hi}$ and $Adm^{+/+}$ mice and saw no observable differences in the levels or expression pattern of Cx43 staining in either sex (Figure II in the online-only Data Supplement). Next, we assessed how *Adm* affects Cx43 in injured hearts. Immunofluorescence of Cx43 through cross-sections of the ventricles revealed notable differences. $Adm^{hi/hi}$ male mice consistently had more Cx43 throughout the section than $Adm^{+/+}$ mice (Figure 4A). At higher magnification, Cx43 was heavily concentrated at the border of the ischemic injury in $Adm^{hi/hi}$ mice (Figure 4B). Costaining with wheat germ agglutinin, a marker of cell borders, revealed that Cx43 retains expression within cell-cell contacts more effectively in $Adm^{hi/hi}$ mice than wild-type mice (Figure 4C). This lateralization phenotype observed in $Adm^{hi/hi}$ mice suggests increased gap junction function as intracellular Cx43 is targeted for degradation in injured cells.

We also found that we could reproduce this lateralization phenotype in cultured embryonic rat atrial cardiomyoblasts (H9c2) cells when treated with AM (Figure III in the online-only Data Supplement). The cells also displayed prominent subcellular lateralization of Cx43, which could be nearly completely abrogated with the treatment of rAM24-50, a competitive inhibitor of AM.

Table 1. Echocardiogram Analysis of *Adm*$^{+/+}$ and *Adm*$^{hi/hi}$ Males Before and After MI

	Baseline		5-Days Post-LAD		10-Days Post-LAD		15-Days Post-LAD	
	Adm$^{+/+}$	*Adm*$^{hi/hi}$	*Adm*$^{+/+}$	*Adm*$^{hi/hi}$	*Adm*$^{+/+}$	*Adm*$^{hi/hi}$	*Adm*$^{+/+}$	*Adm*$^{hi/hi}$
IVS; d, mm	1.17±0.03	1.16±0.03	1.01±0.08	1.27*±0.06	1.03±0.09	1.10±0.11	0.94±0.09	1.29†±0.05
IVS; s, mm	1.87±0.04	1.87±0.03	1.27±0.13	1.67*±0.10	1.36±0.15	1.50±0.16	1.21±0.13	1.95‡±0.08
LVID; d, mm	2.79±0.08	2.99±0.09	4.033±0.20	4.10±0.18	4.07±0.18	3.84±0.20	3.95±0.19	3.60±0.15
LVID; s, mm	1.41±0.07	1.58±0.10	3.25±0.21	3.52±0.25	3.18±0.21	2.84±0.18	3.21±0.23	2.35†±0.20
LVPW; d, mm	1.01±0.03	1.13*±0.05	1.21±0.09	1.05±0.05	1.19±0.07	1.08±0.06	1.32±0.09	1.27±0.14
LVPW; s, mm	1.75±0.06	1.80±0.07	1.46±0.11	1.38±0.06	1.48±0.09	1.47±0.07	1.66±0.11	1.82±0.13
LV mass, mg	112.5±6.06	129.0±7.08	185.0±12.92	214.2±12.41	190.1±10.27	180.4±13.80	191.6±19.35	200.2±21.11
LV mass (corrected), mg	90.04±4.85	103.2±5.66	148.0±10.33	171.4±9.93	152.0±8.22	144.3±11.04	153.3±15.48	160.2±16.89
LV volume; d, μL	30.58±1.86	36.26±2.81	76.21±8.35	70.82±5.92	70.40±6.56	67.13±7.68	70.82±8.15	55.28±5.33
LV volume; s, μL	6.07±0.75	8.25±1.22	48.01±7.04	36.16±4.86	39.17±5.31	33.29±5.11	45.60±7.96	20.84*±3.92
EF, %	81.93±1.62	79.55±1.89	41.04±3.80	48.99±4.05	45.07±3.53	49.40±4.70	39.67±4.13	64.03†±4.61
FS, %	50.55±1.77	48.11±1.95	20.50±2.28	25.27±2.45	22.64±2.07	25.62±2.94	19.46±2.31	35.08†±3.64
Heart rate, BPM	637.7±13.06	603.2±13.67	653.7±17.66	582.2*±24.90	689.7±5.49	598.1†±25.97	685.7±10.76	657.1±20.69
CO (approximately), mL/min, n	15.69±0.94 34	16.81±1.10 27	18.19±1.70 20	20.02±2.11 18	21.44±1.84 18	20.95±3.49 15	17.38±1.86 14	22.50±1.70 8

Data represented as an average±SEM. BPM indicates beats per minutes; CO, cardiac output; d, diastolic; EF, ejection fraction; FS, fractional shortening; IVS, interventricular septal; LAD, left anterior descending ligation; LV, left ventricle; LVID, left ventricle internal diameter; LVPW, left ventricle posterior wall; and s, systole.

*$P \leq 0.05$,

†$P \leq 0.01$,

‡$P \leq 0.001$, by unpaired Student 2-tailed *t* test with Welch correction.

Comparative Expression of Connexin Proteins Within the Cardiac Lymphatic Vasculature in Mice and Humans

Given the ability of AM to regulate Cx43 both in vivo and in vitro in both the myocardium and LECs, we sought to explicitly characterize the expression profile of connexins specifically within the cardiac lymphatic vasculature. Using paraffin sections of human heart tissue obtained from left ventricular assist device implantation surgery, we confirmed that human heart tissue expresses the same connexin proteins as the murine heart (Figure IV in the online-only Data Supplement). Murine paraffin sections were obtained from male hearts after MI. Expression of connexins was evaluated by colocalization with podoplanin, a marker of lymphatic vasculature. Cx43 and Cx47 were both expressed in cardiac lymphatics as evidenced by colocalization of podoplanin in both humans and mouse, while Cx37 was entirely absent from the heart in both mouse and human (Figure IV in the online-only Data Supplement). We further evaluated connexin protein expression in murine hearts by testing uninjured cardiac sections and evaluated staining in both *Adm*$^{hi/hi}$ and *Adm*$^{+/+}$ mice and saw no differences between genotype, nor did expression profile change after MI (data not shown). Overall, human and murine cardiac lymphatics appeared similar in both morphology and density, while also expressing the same connexins.

AM and Verapamil Can Linearize Cx43 and Improve Gap Junction Coupling Within Cultured hLECs Cells

To assess the effect that AM and verapamil have on the function of gap junctions, we performed scrape-loading assays, which permits the gap junction permeable dye, Lucifer yellow, to travel through a cultured monolayer of hLECs after disrupting the monolayer by scraping a needle across the cells. We then visualize and quantify the passage of the dye through the cells in different conditions. As previously published, treatment of hLECs with AM increased gap junction formation, while pretreatment with carbenoxolone, a gap junction inhibitor abrogated gap junction formation (Figure V in the online-only Data Supplement).[39,44]

Interestingly, verapamil, a drug used to treat hypertension and arrhythmias through targeting voltage-gated calcium channels, has recently been shown to have beneficial cardiovascular effects by preserving Cx43 expression.[45] Treatment of hLECs with verapamil had a very similar effect to AM and showed significant increase in gap junction formation (Figure 5A and 5B). To further show that these gap junction coupling phenotypes were a direct result of Cx43 preservation at the cell membrane, we treated hLECs with both AM and verapamil and stained directly for Cx43 (Figure 5C). Both treatments resulted in very similar phenotypes, in which Cx43 localizes to the cell membrane at cell-cell contacts, similar to the lateralization phenotypes we see in vivo. This phenomenon was lost when cells were pretreated with carbenoxolone to inhibit gap junction formation.

Lymphatic-Specific Deletion of Cx43 Results in Defective Permeability and Function of Lymphatic Vasculature That Cannot be Rescued With AM Treatment

To further test the effect of Cx43 on lymphatic function, we generated a lymphatic-specific deletion of Cx43 using

Table 2: Echocardiogram Analysis of *Adm*$^{+/+}$ and *Adm*$^{hi/hi}$ Females Before and After MI

	Baseline		4-Days Post-LAD		10-Days Post-LAD	
	Adm$^{+/+}$	*Adm*$^{hi/hi}$	*Adm*$^{+/+}$	*Adm*$^{hi/hi}$	*Adm*$^{+/+}$	*Adm*$^{hi/hi}$
IVS; d, mm	1.19±0.07	0.94±0.15	1.22±0.8	1.11±0.18	1.09±0.05	1.23±0.06
IVS; s, mm	1.85±0.11	1.60±0.22	1.73±0.16	1.51±0.27	1.51±0.14	1.20*±0.15
LVID; d, mm	2.43±0.18	3.32*±0.22	3.49±0.13	3.85±0.12	3.72±0.28	4.11±0.29
LVID; s, mm	1.20±0.04	1.74±0.35	2.46±0.15	3.04±0.24	2.79±0.21	2.74±0.21
LVPW; d, mm	1.05±0.08	1.05±0.12	1.17±0.12	1.17±0.20	1.14±0.11	1.12±0.17
LVPW; s, mm	1.65±0.09	1.76±0.19	1.53±0.13	1.41±0.15	1.53±0.13	1.54±0.11
LV mass, mg	93.73±11.98	121.4±23.91	168.2±8.63	183.7±16.17	168.0±15.47	210.0±13.00
LV mass (corrected), mg	74.98±9.59	97.14±19.13	134.6±6.91	146.9±12.93	134.4±12.38	168.0±10.40
LV volume; d, μL	21.93±3.99	45.75*±7.21	51.19±4.41	64.06±4.54	62.07±10.45	76.42±11.40
LV volume; s, μL	3.40±0.35	11.01±5.73	22.17±3.27	37.29±7.04	30.80±5.06	28.72±5.14
EF, %	81.02±3.51	78.51±9.09	57.66±3.54	42.87±8.13	48.88±4.80	62.42*±3.18
FS, %	48.89±4.13	48.57±7.73	29.89±2.32	21.22±4.54	24.65±3.07	33.44*±2.34
Heart rate, BPM	712.2±24.86	620.0±42.30	697.9±12.39	675.1±34.78	711.5±8.06	706.5±4.71
CO (approximately), mL/min, n	13.21±2.87 7	21.72±3.96 4	20.30±1.71 7	17.79±2.44 4	22.09±4.68 7	33.63±5.29 4

Data represented as an average±SEM. BPM indicates beats per minutes; CO, cardiac output; d, diastolic; EF, ejection fraction; FS, fractional shortening; IVS, interventricular septal; LAD, left anterior descending ligation; LV, left ventricle; LVID, left ventricle internal diameter; LVPW, left ventricle posterior wall; and s, systole.

*$P \leq 0.05$, by unpaired Student 2-tailed *t* test with Welch correction.

inducible Vegfr3-CreER (T2). To test the effects of Cx43 on permeability of lymphatic vessels, we used Evans Blue Dye which can penetrate dermal lymphatics. Injection of 0.5% Evans Blue intradermally in the ear showed rapid uptake in ear dermal lymphatics in *Vegfr3-CreER*^{T2}*; Cx43*$^{fl/fl}$ and control mice (Figure 6A). However, after 5 minutes diffusion of the dye was largely exacerbated in *Vegfr3-CreER*^{T2}; *Cx43*$^{fl/fl}$ mice compared with control mice. After 15 minutes, the diffusion of the dye persisted significantly in the *Vegfr3-CreER*^{T2}; *Cx43*$^{fl/fl}$ mice.

We further tested permeability and function of dermal tail lymphatic vasculature by assessing in vivo lymphatic tail flow using fluorescent tail microlymphography in adult mice. Briefly, fluorescein isothiocyanate dextran, a fluorescent dye, was injected directly into the interstitial space of the tail in the presence or absence of AM in *Vegfr3-CreER*^{T2}; *Cx43*$^{fl/fl}$ and control mice. The ability of the dye to enter and flow through lymphatic capillaries was monitored over time. *Vegfr3-CreER*^{T2}; *Cx43*$^{fl/fl}$ mice have lymphatic velocities nearly double that of control mice (Figure 6B). Consistent with previously published data, control mice had a slight but significant decrease in lymphatic velocity when coinjected with AM[13] (Figure 6B). However, in mice lacking Cx43, AM had no effect on lymphatic tail velocity. As summarized in Table I in the online-only Data Supplement, individual lymphatic tail vasculature vessels were analyzed for morphology changes and changes in intensity of dye over time. Although morphology remained unchanged between genotypes or treatment groups over time (6–7 minutes postinjection), control mice had a reduction in dye intensity (at 3 and 6 minutes postinjection) with AM treatment suggesting a reduction in dye volume within the individual lymphatic capillaries, consistent with the reduction in velocity. *Vegfr3-CreER*^{T2}; *Cx43*$^{fl/fl}$ mice had no such effects with AM treatment; morphology and dye intensity remained constant over time with treatment.

We know that AM stabilizes endothelial junctions in LECs.[13,40] It has previously been published that Cx43 and ZO-1 (zonula occluden-1) are bound at cell-cell junctions in the heart.[46] We confirmed this interaction in a proximal ligation assay in untreated hLECs, an assay that tests for protein-protein interactions based on proximity between the proteins (Figure 6C). In some physiological conditions, like MI, ZO-1 has a higher affinity for c-Src (proto-oncogene tyrosine-protein kinase Src) than Cx43.[46] This causes Cx43 to disassociate from the cell membrane, making the gap junction nonfunctional.[46,47] We treated hLECs with AM and stained for both Cx43 and ZO-1 (Figure 6D). Cells treated with AM showed more continuous ZO-1 junctions and increased Cx43 at the cell-cell membrane contacts compared with vehicle-treated cells. We propose a model in which AM stabilizes the binding of Cx43 and ZO-1 and endothelial junctions in LECs (Figure 6E).

Discussion

It has recently been established that cardiac lymphangiogenesis and lymphatic remodeling is a common response to myocardial injury and cardiac diseases, yet the exact mechanisms regulating this phenomenon remain to be completely understood.[9–11] These vessels are primarily responsible for regulating fluid transport and trafficking of immune cells to clear edema and resolve inflammation, especially after MI.[5,48] To further complicate such an intricate process, sex differences are prevalent but often underrepresented in cardiovascular disease-related research. Anatomy, hormones, physiology, and cell signaling of

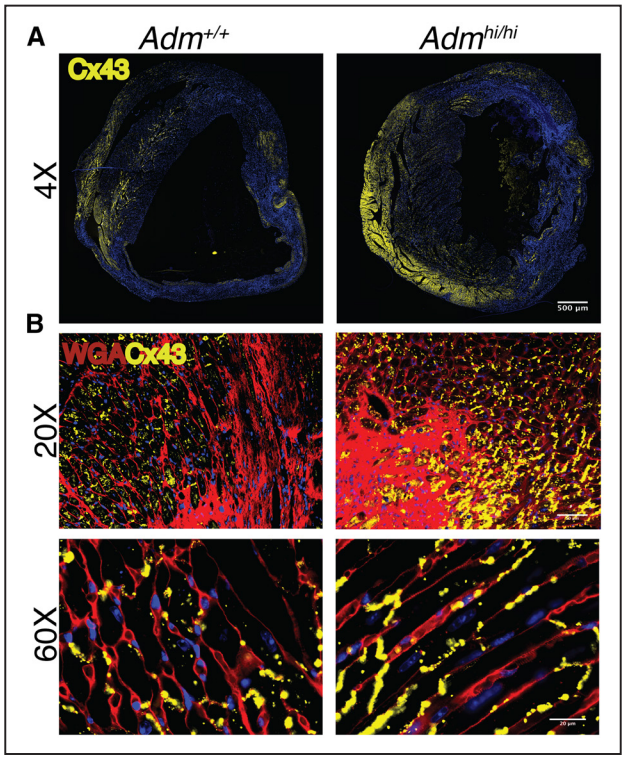

Figure 4. Adrenomedullin *(Adm)* affects localization of Cx43 (connexin 43) in injured myocardium. A, Immunohistochemistry of cardiac sections in infarcted adult male *Adm*$^{+/+}$ and *Adm*$^{hi/hi}$ 10–15 d post-MI (yellow=Cx43, blue=Hoescht); scale bar=500 μm. **B**, Immunohistochemistry of cardiac sections in peri-infarct zone of adult male *Adm*$^{+/+}$ and *Adm*$^{hi/hi}$ mice 10–15 d post-MI (yellow=Cx43, red=wheat germ agglutinin [WGA], blue=Hoescht); scale bar=50 and 20 μm.

the heart and its vasculature differ significantly between males and females.[49] In this study, we show for the first time that cardiac lymphatics have innate differences between the sexes.

Finding effective endogenous factors that positively regulate the cardiovascular healing process through lymphangiogenesis has been challenging. For example, VEGF (vascular endothelial growth factor)-C induced lymphangiogenesis alone may not be enough to repair the post-MI heart.[10] AM levels increase endogenously in response to cardiac injury and disease, including MI.[50] Exogenous AM treatment has frequently been shown to be cardioprotective, but the exact mechanisms regulating this process are very dependent on experimental conditions.[51–53] The *Adm*$^{hi/hi}$ mouse model allows us to study the effect of global, constitutive overexpression of *Adm* for the first time without confounding factors such as injection time, dose, or viral delivery methods. We show that overexpression of *Adm* is not only sufficient to drive a proliferative response in cardiac lymphatic vasculature in both males and females, but also improve cardiac function 1 to 2 weeks after MI while suppressing cardiac edema. Given that increases in cardiac edema as small as 2% can have profound effects on cardiac output, this could be an extremely valuable therapeutic discovery.[54,55] Overall, echocardiogram results, histology, and quantification of cardiac lymphatic vessels indicate that *Adm*$^{hi/hi}$ mice retain less fluid and undergo less remodeling, which likely can be attributed to the difference in lymphatic vasculature since infarct size remains unchanged.

Resolution of cardiac edema has previously been shown to be bimodal with peak increases in water content happening 3 hours after MI and resolving by 24 hours and a second peak happening 7 days after MI.[56] These studies though valuable were done using only male animal models. Our studies reveal interesting differences in the timing of cardiac edema resolution between males and females. Although we see very similar cardiac lymphatic vasculature by 15 days after MI in both male and female mice, improvements in cardiac function (ejection fraction and fractional shortening) are seen a full 5 days sooner in female mice. We also see profound differences in the resolution of hind paw edema between males and females; *Adm*$^{hi/hi}$ females show significant improvement 1-day post-CFA injection, while *Adm*$^{hi/hi}$ males see no significant improvement for 6 days. This may be because of developmental

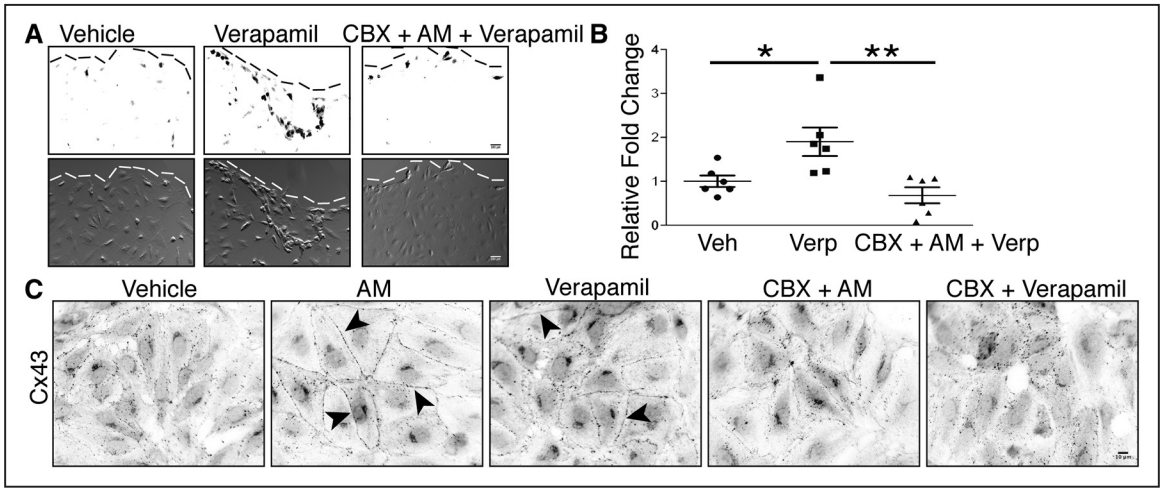

Figure 5. AM (adrenomedullin) and verapamil can linearize Cx43 (connexin 43) and improve gap junction coupling within cultured human lymphatic endothelial (hLECs) cells. A, Transfer of Lucifer yellow dye through hLECs was imaged after scrape loading. Cells were pretreated with gap junction inhibitor carbenoxolone (CBX; 100 μM) for 30 min followed by treatment with verapamil (10 μM) for 15 min; scale bar=50 μm. **B**, The percentage of dye-coupled cells was quantified by dividing the number of Lucifer yellow-positive cells by the total number of cells in the field using Image J threshold. *P<0.05, **P<0.01 by Tukey multiple comparisons test 1-way ANOVA. Mean±SEM is shown. **C**, Cx43 expression and localization in response to AM and verapamil treatment. hLECs were pretreated with CBX (100 μM) for 30 min followed by treatment with hAM (10 nM) or verapamil (10 μM) for 15 min and stained for Cx43. Arrows highlight Cx43 at cell-cell contacts; scale bar=10 μm.

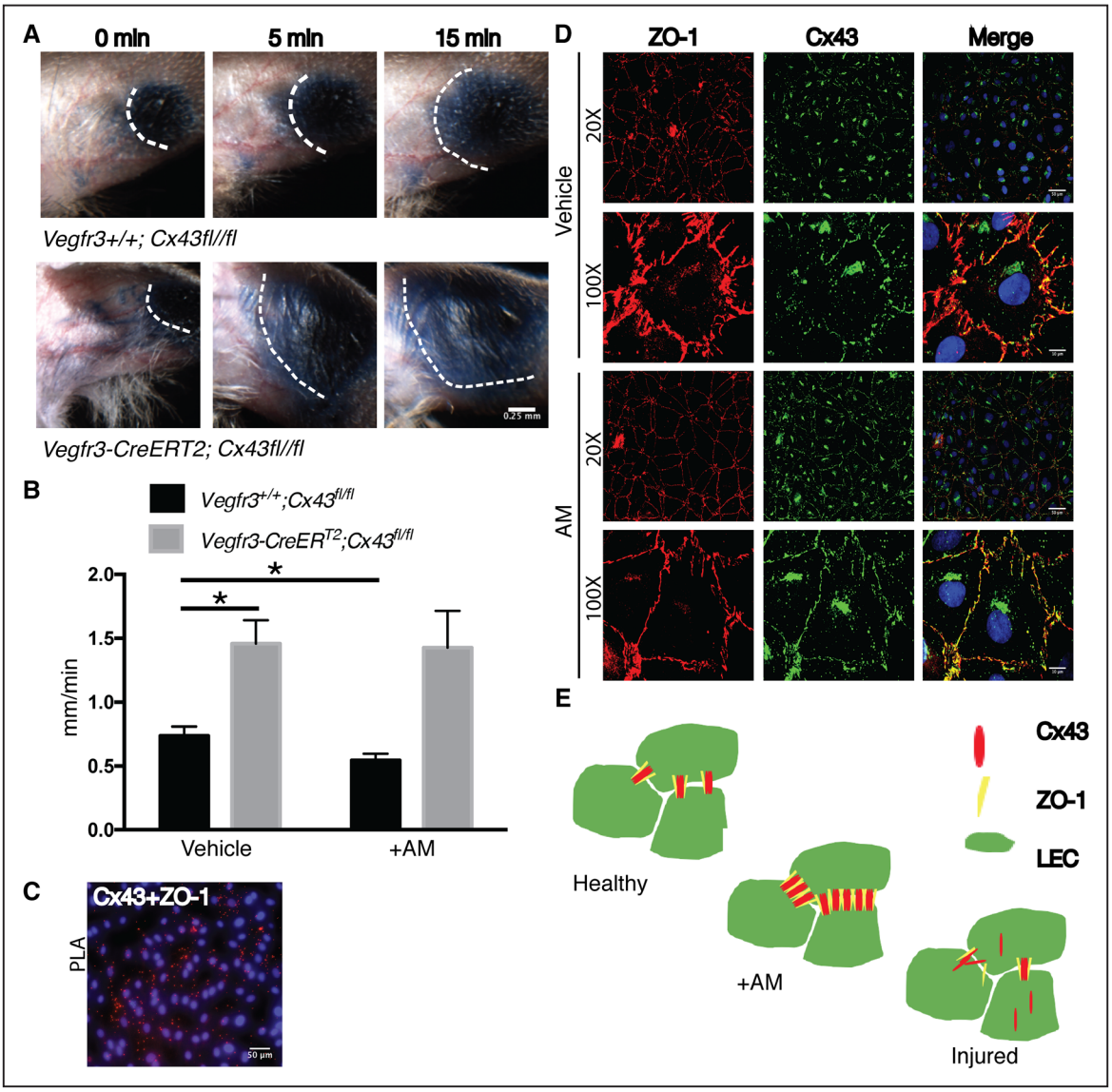

Figure 6. Lymphatic-specific Cx43 (connexin 43) deletion leads to defective lymphatic vessels; AM (adrenomedullin) targets Cx43 to tighten and linearize junctions in lymphatic endothelial cells (LECs). A, In vivo lymphatic permeability assay assessing the leakage of Evans blue dye from the dermal lymphatic vessels in the ear. Images represent Evan's blue dye location directly after the injection of the dye, 5 min, and 15 min postinjection; scale bar=0.25 mm. **B**, In vivo tail microlymphography assessed velocity of dye transport in tail lymphatics with and without AM coinjection. *P<0.05 by unpaired Student 2-tailed t test with Welch correction. Mean±SEM is shown. **C**, PLA (proximal ligation assay) Cx43 and ZO-1 (zonula occluden-1) interaction in human LECs (hLECs); scale bar=50 µm. **D**, Cx43 and ZO-1 expression and localization in response to hAM (10 nM) treatment for 15 min; scale bar=50 and 10 µm. **E**, AM increases Cx43 and ZO-1 interactions in LECs.

differences in cardiac lymphatic vasculature or other factors, like estrogen. Premenopausal women are innately protected from cardiovascular disease and heart failure, likely in part due to estrogen.[57] *Adm* expression can be induced by estrogen and is likely regulated via estrogen-induced miRNAs.[43,58] Further studies are needed to fully characterize how sex differences impact the lymphangiogenic repair process.

Previous studies have established that the main source of AM driving cardiac proliferation during development originates from the epicardium.[42,59] Reactivation of the epicardium is known to be involved in cardiac remodeling and scar formation after myocardial injury through secretion of paracrine factors.[60] Our results further emphasize the importance of the epicardium in cardiac healing and remodeling after injury, while highlighting a novel role in cardiac lymphatic regulation. Like previous studies we see the majority of de novo vessels forming in the peri-infarct zone near the epicardium or the epicardial border zone.[61] This paracrine signaling results not only in more vessels in $Adm^{hi/hi}$ mice, but the vessels are larger and more dilated indicative of differences in function.

Previous studies have characterized the importance of Cx37, Cx47, and Cx43 as the main connexin proteins expressed in developing lymphatic tissue.[62,63] Mutations in these genes lead to lymphatic disorders in both mice and humans.[27,28,30–32] Gap junction intercellular communication is involved in proper contraction of lymph vessels through the spreading of polarization currents.[64] However, it remains unknown what connexin proteins are expressed in the lymphatic vasculature specifically within the heart. Recent work showed

that lymphatic cells within the heart have a unique, heterogeneous genetic origin that likely differs from other lymphatic systems.[9] We show here that Cx47 and Cx43 are expressed in the cardiac lymphatic vasculature, while Cx37 is notably absent from the lymphatic vessels in the heart in both murine and human tissue, making mice an ideal model for these studies. Mouse models with inducible lymphatic-specific deletion of Cx43 emphasize the requirement of Cx43 not only in development but maintenance of lymphatic function and also strengthen our findings that AM targets Cx43. Further characterization of how connexins regulate these vessels would be incredibly beneficial to fully unlocking the potential of targeting cardiac lymphatics as a therapeutic avenue.

It is already known that AM does not seem to affect expression or localization of Cx37 or Cx47 in vitro, but has the ability to increase mRNA and protein levels of Cx43 in hLECs while improving gap junction coupling function.[39] In our study, the increase in AM correlates to an overall elevation of Cx43 but more interestingly specific localization within cardiac LECs with preservation at the cell membrane. The previously characterized lateralization phenotype we see is associated with increased survival, increased cardiac conduction, and Cx43 stability.[65–67] During ischemia in the heart, the deprivation of oxygen within the cell lowers the pH and causes Cx43 to be targeted for degradation leading to consequences including arrhythmia.[46,47] The role of Cx43 in electrical conduction of the heart is well established, and the lateralization of Cx43 is likely contributing to the increase in cardiac contractile function in border and remote zones, having a synergistic effect on the function of lymphatic vessels, which rely on cardiac contractions for effective lymph flow.

Verapamil is a drug that has been used to treat hypertension and arrhythmias through direct targeting of L-type calcium channels.[68] However, it has also been shown to have indirect effects on the localization and stabilization of Cx43. By inhibiting calcium influx and preserving oxygen levels in the heart with verapamil, Cx43 is stabilized during injury resulting in beneficial antiarrhythmic phenotypes.[45] We used hLECs to show that verapamil has a similarly positive effect on the lateralization of Cx43 in lymphatics as it does in cardiomyocytes. Verapamil also had a positive effect on gap junction coupling in vitro. This discovery is a previously uncharacterized benefit of verapamil therapy for cardiac lymphatic function. AM was just as effective at gap junction coupling as verapamil in hLECs. As a protein that signals through a GPCR (G-protein coupled receptor), CLR (calcitonin receptor-like receptor; *Calcrl*=gene) with specific coreceptor RAMP2 (receptor-activity modifying protein 2), adrenomedullin is an ideal candidate for a druggable biological target.[69]

In conclusion, our data show an endogenous lymphangiogenic response that is augmented by overexpression of *Adm*. We show that AM and verapamil can target Cx43 to increase gap junction coupling between hLECs. Our work highlights previously uncharacterized pathways and sex differences involved in cardiac lymphangiogenesis that preserve cardiac function and reduce edema. Further exploration of these and other factors could have profoundly beneficial effects in patients experiencing MI or other cardiovascular ailments.

Acknowledgments

We thank the University of North Carolina Animal Models Core, the University of North Carolina MHI (McAllister Heart Institute) Animal Surgery Core Lab, the University of North Carolina Histology Research Core, the University of North Carolina CGIBD (Center for Gastrointestinal Biology & Disease) Histology core, the University of North Carolina Hooker Imaging Core, and the University of North Carolina Microscopy Services Laboratory. We thank Dr Sagrario Ortega for the use of the Vegfr3-CreER (T2) mice. We also thank Drs James Faber, Pablo Ariel, Daniel Kechele, and members of the Caron laboratory for technical support and discussions.

Sources of Funding

This work was supported by National Institutes of Health grants HL129086 to K. Caron and an American Heart Association Innovator Award 161RG27260077 to K. Caron, predoctoral grant 15PRE25680001 to C. Trincot, and Swiss National Science Foundation grant 31ER30-160674 to T. Petrova. The Microscopy Services Laboratory, Department of Pathology and Laboratory Medicine, is supported in part by P30 CA016086 Cancer Center Core Support Grant to the University of North Carolina Lineberger Comprehensive Cancer Center. Research reported in this publication was supported in part by the North Carolina Biotech Center Institutional Support Grant 2016-IDG-1016.

Disclosures

None.

References

1. Alitalo K. The lymphatic vasculature in disease. *Nat Med*. 2011;17:1371–1380. doi: 10.1038/nm.2545
2. Schulte-Merker S, Sabine A, Petrova TV. Lymphatic vascular morphogenesis in development, physiology, and disease. *J Cell Biol*. 2011;193:607–618. doi: 10.1083/jcb.201012094
3. Bradham RR, Parker EF, Barrington BA Jr, Webb CM, Stallworth JM. The cardiac lymphatics. *Ann Surg*. 1970;171:899–902.
4. Aspelund A, Robciuc MR, Karaman S, Makinen T, Alitalo K. Lymphatic system in cardiovascular medicine. *Circ Res*. 2016;118:515–530. doi: 10.1161/CIRCRESAHA.115.306544
5. Vieira JM, Norman S, Villa Del Campo C, Cahill TJ, Barnette DN, Gunadasa-Rohling M, Johnson LA, Greaves DR, Carr CA, Jackson DG, Riley PR. The cardiac lymphatic system stimulates resolution of inflammation following myocardial infarction. *J Clin Invest*. 2018;128:3402–3412. doi: 10.1172/JCI97192
6. Davis KL, Laine GA, Geissler HJ, Mehlhorn U, Brennan M, Allen SJ. Effects of myocardial edema on the development of myocardial interstitial fibrosis. *Microcirculation*. 2000;7:269–280.
7. Anand IS, Ferrari R, Kalra GS, Wahi PL, Poole-Wilson PA, Harris PC. Edema of cardiac origin. Studies of body water and sodium, renal function, hemodynamic indexes, and plasma hormones in untreated congestive cardiac failure. *Circulation*. 1989;80:299–305.
8. Zia MI, Ghugre NR, Connelly KA, Strauss BH, Sparkes JD, Dick AJ, Wright GA. Characterizing myocardial edema and hemorrhage using quantitative T2 and T2* mapping at multiple time intervals post ST-segment elevation myocardial infarction. *Circ Cardiovasc Imaging*. 2012;5:566–572. doi: 10.1161/CIRCIMAGING.112.973222
9. Klotz L, Norman S, Vieira JM, Masters M, Rohling M, Dubé KN, Bollini S, Matsuzaki F, Carr CA, Riley PR. Cardiac lymphatics are heterogeneous in origin and respond to injury. *Nature*. 2015;522:62–67. doi: 10.1038/nature14483
10. Henri O, Pouehe C, Houssari M, Galas L, Nicol L, Edwards-Lévy F, Henry JP, Dumesnil A, Boukhalfa I, Banquet S, Schapman D, Thuillez C, Richard V, Mulder P, Brakenhielm E. Selective stimulation of cardiac lymphangiogenesis reduces myocardial edema and fibrosis leading to improved cardiac function following myocardial infarction. *Circulation*. 2016;133:1484–1497; discussion 1497. doi: 10.1161/CIRCULATIONAHA.115.020143
11. Tatin F, Renaud-Gabardos E, Godet AC, Hantelys F, Pujol F, Morfoisse F, Calise D, Viars F, Valet P, Masri B, Prats AC, Garmy-Susini B. Apelin modulates pathological remodeling of lymphatic endothelium after myocardial infarction. *JCI Insight*. 2017;2:93887. doi: 10.1172/jci.insight.93887

12. Caron KM, Smithies O. Extreme hydrops fetalis and cardiovascular abnormalities in mice lacking a functional Adrenomedullin gene. *Proc Natl Acad Sci USA*. 2001;98:615–619. doi: 10.1073/pnas.021548898
13. Dunworth WP, Fritz-Six KL, Caron KM. Adrenomedullin stabilizes the lymphatic endothelial barrier in vitro and in vivo. *Peptides*. 2008;29:2243–2249. doi: 10.1016/j.peptides.2008.09.009
14. Kataoka Y, Miyazaki S, Yasuda S, Nagaya N, Noguchi T, Yamada N, Morii I, Kawamura A, Doi K, Miyatake K, Tomoike H, Kangawa K. The first clinical pilot study of intravenous adrenomedullin administration in patients with acute myocardial infarction. *J Cardiovasc Pharmacol*. 2010;56:413–419. doi: 10.1097/FJC.0b013e3181f15b45
15. Maisel A, Mueller C, Nowak R, et al. Mid-region pro-hormone markers for diagnosis and prognosis in acute dyspnea: results from the BACH (Biomarkers in Acute Heart Failure) trial. *J Am Coll Cardiol*. 2010;55:2062–2076. doi: 10.1016/j.jacc.2010.02.025
16. Morbach C, Marx A, Kaspar M, Güder G, Brenner S, Feldmann C, Störk S, Vollert JO, Ertl G, Angermann CE; INH Study Group and the Competence Network Heart Failure. Prognostic potential of midregional pro-adrenomedullin following decompensation for systolic heart failure: comparison with cardiac natriuretic peptides. *Eur J Heart Fail*. 2017;19:1166–1175. doi: 10.1002/ejhf.859
17. Jougasaki M, Burnett JC Jr. Adrenomedullin: potential in physiology and pathophysiology. *Life Sci*. 2000;66:855–872.
18. Meens MJ, Kwak BR, Duffy HS. Role of connexins and pannexins in cardiovascular physiology. *Cell Mol Life Sci*. 2015;72:2779–2792. doi: 10.1007/s00018-015-1959-2
19. Söhl G, Willecke K. Gap junctions and the connexin protein family. *Cardiovasc Res*. 2004;62:228–232. doi: 10.1016/j.cardiores.2003.11.013
20. Unger VM, Kumar NM, Gilula NB, Yeager M. Three-dimensional structure of a recombinant gap junction membrane channel. *Science*. 1999;283:1176–1180.
21. Alexander DB, Goldberg GS. Transfer of biologically important molecules between cells through gap junction channels. *Curr Med Chem*. 2003;10:2045–2058.
22. Zong L, Zhu Y, Liang R, Zhao HB. Gap junction mediated miRNA intercellular transfer and gene regulation: a novel mechanism for intercellular genetic communication. *Sci Rep*. 2016;6:19884. doi: 10.1038/srep19884
23. Cherian PP, Cheng B, Gu S, Sprague E, Bonewald LF, Jiang JX. Effects of mechanical strain on the function of gap junctions in osteocytes are mediated through the prostaglandin EP2 receptor. *J Biol Chem*. 2003;278:43146–43156. doi: 10.1074/jbc.M302993200
24. Ongstad EL, O'Quinn MP, Ghatnekar GS, Yost MJ, Gourdie RG. A connexin43 mimetic peptide promotes regenerative healing and improves mechanical properties in skin and heart. *Adv Wound Care (New Rochelle)*. 2013;2:55–62. doi: 10.1089/wound.2011.0341
25. Roell W, Lewalter T, Sasse P, et al. Engraftment of connexin 43-expressing cells prevents post-infarct arrhythmia. *Nature*. 2007;450:819–824. doi: 10.1038/nature06321
26. Fernandes S, van Rijen HV, Forest V, Evain S, Leblond AL, Mérot J, Charpentier F, de Bakker JM, Lemarchand P. Cardiac cell therapy: overexpression of connexin43 in skeletal myoblasts and prevention of ventricular arrhythmias. *J Cell Mol Med*. 2009;13:3703–3712. doi: 10.1111/j.1582-4934.2009.00740.x
27. Kanady JD, Dellinger MT, Munger SJ, Witte MH, Simon AM. Connexin37 and connexin43 deficiencies in mice disrupt lymphatic valve development and result in lymphatic disorders including lymphedema and chylothorax. *Dev Biol*. 2011;354:253–266. doi: 10.1016/j.ydbio.2011.04.004
28. Munger SJ, Davis MJ, Simon AM. Defective lymphatic valve development and chylothorax in mice with a lymphatic-specific deletion of connexin43. *Dev Biol*. 2017;421:204–218. doi: 10.1016/j.ydbio.2016.11.017
29. Glass AM, Snyder EG, Taffet SM. Connexins and pannexins in the immune system and lymphatic organs. *Cell Mol Life Sci*. 2015;72:2899–2910. doi: 10.1007/s00018-015-1966-3
30. Brice G, Ostergaard P, Jeffery S, Gordon K, Mortimer PS, Mansour S. A novel mutation in GJA1 causing oculodentodigital syndrome and primary lymphoedema in a three generation family. *Clin Genet*. 2013;84:378–381. doi: 10.1111/cge.12158
31. Ferrell RE, Baty CJ, Kimak MA, Karlsson JM, Lawrence EC, Franke-Snyder M, Meriney SD, Feingold E, Finegold DN. GJC2 missense mutations cause human lymphedema. *Am J Hum Genet*. 2010;86:943–948. doi: 10.1016/j.ajhg.2010.04.010
32. Finegold DN, Baty CJ, Knickelbein KZ, Perschke S, Noon SE, Campbell D, Karlsson JM, Huang D, Kimak MA, Lawrence EC, Feingold E, Meriney SD, Brufsky AM, Ferrell RE. Connexin 47 mutations increase risk for secondary lymphedema following breast cancer treatment. *Clin Cancer Res*. 2012;18:2382–2390. doi: 10.1158/1078-0432.CCR-11-2303
33. Li M, Schwerbrock NM, Lenhart PM, Fritz-Six KL, Kadmiel M, Christine KS, Kraus DM, Espenschied ST, Willcockson HH, Mack CP, Caron KM. Fetal-derived adrenomedullin mediates the innate immune milieu of the placenta. *J Clin Invest*. 2013;123:2408–2420. doi: 10.1172/JCI67039
34. Liao Y, Day KH, Damon DN, Duling BR. Endothelial cell-specific knockout of connexin 43 causes hypotension and bradycardia in mice. *Proc Natl Acad Sci USA*. 2001;98:9989–9994. doi: 10.1073/pnas.171305298
35. Martinez-Corral I, Stanczuk L, Frye M, Ulvmar MH, Diéguez-Hurtado R, Olmeda D, Makinen T, Ortega S. Vegfr3-CreER (T2) mouse, a new genetic tool for targeting the lymphatic system. *Angiogenesis*. 2016;19:433–445. doi: 10.1007/s10456-016-9505-x
36. Renier N, Wu Z, Simon DJ, Yang J, Ariel P, Tessier-Lavigne M. iDISCO: a simple, rapid method to immunolabel large tissue samples for volume imaging. *Cell*. 2014;159:896–910. doi: 10.1016/j.cell.2014.10.010
37. Kechele DO, Dunworth WP, Trincot CE, Wetzel-Strong SE, Li M, Ma H, Liu J, Caron KM. Endothelial restoration of receptor activity-modifying protein 2 is sufficient to rescue lethality, but survivors develop dilated cardiomyopathy. *Hypertension*. 2016;68:667–677. doi: 10.1161/HYPERTENSIONAHA.116.07191
38. Takagawa J, Zhang Y, Wong ML, Sievers RE, Kapasi NK, Wang Y, Yeghiazarians Y, Lee RJ, Grossman W, Springer ML. Myocardial infarct size measurement in the mouse chronic infarction model: comparison of area- and length-based approaches. *J Appl Physiol (1985)*. 2007;102:2104–2111. doi: 10.1152/japplphysiol.00033.2007
39. Karpinich NO, Caron KM. Gap junction coupling is required for tumor cell migration through lymphatic endothelium. *Arterioscler Thromb Vasc Biol*. 2015;35:1147–1155. doi: 10.1161/ATVBAHA.114.304752
40. Hoopes SL, Willcockson HH, Caron KM. Characteristics of multi-organ lymphangiectasia resulting from temporal deletion of calcitonin receptor-like receptor in adult mice. *PLoS One*. 2012;7:e45261. doi: 10.1371/journal.pone.0045261
41. Ratajska A, Gula G, Flaht-Zabost A, Czarnowska E, Ciszek B, Jankowska-Steifer E, Niderla-Bielinska J, Radomska-Lesniewska D. Comparative and developmental anatomy of cardiac lymphatics. *ScientificWorldJournal*. 2014;2014:183170. doi: 10.1155/2014/183170
42. Wetzel-Strong SE, Li M, Klein KR, Nishikimi T, Caron KM. Epicardial-derived adrenomedullin drives cardiac hyperplasia during embryogenesis. *Dev Dyn*. 2014;243:243–256. doi: 10.1002/dvdy.24065
43. Wetzel-Strong SE, Li M, Espenschied ST, Caron KM. Cohort of estrogen-induced microRNAs regulate adrenomedullin expression. *Am J Physiol Regul Integr Comp Physiol*. 2016;310:R209–R216. doi:10.1152/ajpregu.00305.2014
44. Goldberg GS, Moreno AP, Bechberger JF, Hearn SS, Shivers RR, MacPhee DJ, Zhang YC, Naus CC. Evidence that disruption of connexon particle arrangements in gap junction plaques is associated with inhibition of gap junctional communication by a glycyrrhetinic acid derivative. *Exp Cell Res*. 1996;222:48–53. doi: 10.1006/excr.1996.0006
45. Zhou P, Zhang SM, Wang QL, Wu Q, Chen M, Pei JM. Anti-arrhythmic effect of verapamil is accompanied by preservation of cx43 protein in rat heart. *PLoS One*. 2013;8:e71567. doi: 10.1371/journal.pone.0071567
46. Kieken F, Mutsaers N, Dolmatova E, Virgil K, Wit AL, Kellezi A, Hirst-Jensen BJ, Duffy HS, Sorgen PL. Structural and molecular mechanisms of gap junction remodeling in epicardial border zone myocytes following myocardial infarction. *Circ Res*. 2009;104:1103–1112. doi: 10.1161/CIRCRESAHA.108.190454
47. Matsushita T, Oyamada M, Fujimoto K, Yasuda Y, Masuda S, Wada Y, Oka T, Takamatsu T. Remodeling of cell-cell and cell-extracellular matrix interactions at the border zone of rat myocardial infarcts. *Circ Res*. 1999;85:1046–1055.
48. Cahill TJ, Choudhury RP, Riley PR. Heart regeneration and repair after myocardial infarction: translational opportunities for novel therapeutics. *Nat Rev Drug Discov*. 2017;16:699–717. doi: 10.1038/nrd.2017.106
49. Boese AC, Kim SC, Yin KJ, Lee JP, Hamblin MH. Sex differences in vascular physiology and pathophysiology: estrogen and androgen signaling in health and disease. *Am J Physiol Heart Circ Physiol*. 2017;313:H524–H545. doi: 10.1152/ajpheart.00217.2016
50. Gibbons C, Dackor R, Dunworth W, Fritz-Six K, Caron KM. Receptor activity-modifying proteins: RAMPing up adrenomedullin signaling. *Mol Endocrinol*. 2007;21:783–796. doi: 10.1210/me.2006-0156
51. Hamid SA, Totzeck M, Drexhage C, Thompson I, Fowkes RC, Rassaf T, Baxter GF. Nitric oxide/cGMP signalling mediates the cardioprotective action of adrenomedullin in reperfused myocardium. *Basic Res Cardiol*. 2010;105:257–266. doi: 10.1007/s00395-009-0058-7

52. Kato K, Yin H, Agata J, Yoshida H, Chao L, Chao J. Adrenomedullin gene delivery attenuates myocardial infarction and apoptosis after ischemia and reperfusion. *Am J Physiol Heart Circ Physiol*. 2003;285:H1506–H1514. doi: 10.1152/ajpheart.00270.2003
53. Wei X, Zhao C, Jiang J, Li J, Xiao X, Wang DW. Adrenomedullin gene delivery alleviates hypertension and its secondary injuries of cardiovascular system. *Hum Gene Ther*. 2005;16:372–380. doi: 10.1089/hum.2005.16.372
54. Laine GA, Allen SJ. Left ventricular myocardial edema. Lymph flow, interstitial fibrosis, and cardiac function. *Circ Res*. 1991;68:1713–1721.
55. Dongaonkar RM, Stewart RH, Geissler HJ, Laine GA. Myocardial microvascular permeability, interstitial oedema, and compromised cardiac function. *Cardiovasc Res*. 2010;87:331–339. doi: 10.1093/cvr/cvq145
56. Fernández-Jiménez R, Sánchez-González J, Agüero J, et al. Myocardial edema after ischemia/reperfusion is not stable and follows a bimodal pattern: imaging and histological tissue characterization. *J Am Coll Cardiol*. 2015;65:315–323. doi: 10.1016/j.jacc.2014.11.004
57. Moolman JA. Unravelling the cardioprotective mechanism of action of estrogens. *Cardiovasc Res*. 2006;69:777–780.
58. Watanabe H, Takahashi E, Kobayashi M, Goto M, Krust A, Chambon P, Iguchi T. The estrogen-responsive adrenomedullin and receptor-modifying protein 3 gene identified by DNA microarray analysis are directly regulated by estrogen receptor. *J Mol Endocrinol*. 2006;36:81–89. doi: 10.1677/jme.1.01825
59. Klein KR, Karpinich NO, Espenschied ST, Willcockson HH, Dunworth WP, Hoopes SL, Kushner EJ, Bautch VL, Caron KM. Decoy receptor CXCR7 modulates adrenomedullin-mediated cardiac and lymphatic vascular development. *Dev Cell*. 2014;30:528–540. doi: 10.1016/j.devcel.2014.07.012
60. Zhou B, Honor LB, He H, et al. Adult mouse epicardium modulates myocardial injury by secreting paracrine factors. *J Clin Invest*. 2011;121:1894–1904. doi: 10.1172/JCI45529
61. Sun QN, Wang YF, Guo ZK. Reconstitution of myocardial lymphatic vessels after acute infarction of rat heart. *Lymphology*. 2012;45:80–86.
62. Munger SJ, Geng X, Srinivasan RS, Witte MH, Paul DL, Simon AM. Segregated Foxc2, NFATc1 and Connexin expression at normal developing venous valves, and Connexin-specific differences in the valve phenotypes of Cx37, Cx43, and Cx47 knockout mice. *Dev Biol*. 2016;412:173–190. doi: 10.1016/j.ydbio.2016.02.033
63. Sabine A, Agalarov Y, Maby-El Hajjami H, et al. Mechanotransduction, PROX1, and FOXC2 cooperate to control connexin37 and calcineurin during lymphatic-valve formation. *Dev Cell*. 2012;22:430–445. doi: 10.1016/j.devcel.2011.12.020
64. Zawieja DC, Davis KL, Schuster R, Hinds WM, Granger HJ. Distribution, propagation, and coordination of contractile activity in lymphatics. *Am J Physiol*. 1993;264:H1283–H1291. doi: 10.1152/ajpheart.1993.264.4.H1283
65. Qu J, Volpicelli FM, Garcia LI, Sandeep N, Zhang J, Márquez-Rosado L, Lampe PD, Fishman GI. Gap junction remodeling and spironolactone-dependent reverse remodeling in the hypertrophied heart. *Circ Res*. 2009;104:365–371. doi: 10.1161/CIRCRESAHA.108.184044
66. Peters NS, Coromilas J, Severs NJ, Wit AL. Disturbed connexin43 gap junction distribution correlates with the location of reentrant circuits in the epicardial border zone of healing canine infarcts that cause ventricular tachycardia. *Circulation*. 1997;95:988–996.
67. Chkourko HS, Guerrero-Serna G, Lin X, Darwish N, Pohlmann JR, Cook KE, Martens JR, Rothenberg E, Musa H, Delmar M. Remodeling of mechanical junctions and of microtubule-associated proteins accompany cardiac connexin43 lateralization. *Heart Rhythm*. 2012;9:1133–1140.e6. doi: 10.1016/j.hrthm.2012.03.003
68. Curtis MJ, Walker MJ. The mechanism of action of the optical enantiomers of verapamil against ischaemia-induced arrhythmias in the conscious rat. *Br J Pharmacol*. 1986;89:137–147.
69. McLatchie LM, Fraser NJ, Main MJ, Wise A, Brown J, Thompson N, Solari R, Lee MG, Foord SM. RAMPs regulate the transport and ligand specificity of the calcitonin-receptor-like receptor. *Nature*. 1998;393:333–339. doi: 10.1038/30666